First-principles calculations of transition metal solute interactions with hydrogen in tungsten

2016 Nucl. Fusion 56 026004

(http://iopscience.iop.org/0029-5515/56/2/026004)

IOP Publishing | International Atomic Energy Agency Nuclear Fusion

Nucl. Fusion **56** (2016) 026004 (14pp) doi:10.1088/0029-5515/56/2/026004

First-principles calculations of transition metal solute interactions with hydrogen in tungsten

Xiang-Shan Kong[1], Xuebang Wu[1], C.S. Liu[1], Q.F. Fang[1], Q.M. Hu[2], Jun-Ling Chen[3] and G.-N. Luo[3]

[1] Key Laboratory of Materials Physics, Institute of Solid State Physics, Chinese Academy of Sciences, Hefei 230031, People's Republic of China
[2] Shenyang National Laboratory for Materials Science, Institute of Metal Research, Chinese Academy of Sciences, Shenyang 110016, People's Republic of China
[3] Institute of Plasma Physics, Chinese Academy of Sciences, Hefei 230031, People's Republic of China

E-mail: csliu@issp.ac.cn and qmhu@imr.ac.cn

Received 4 May 2015, revised 22 September 2015
Accepted for publication 16 November 2015
Published 30 December 2015

Abstract

We have performed systematic first-principles calculations to predict the interaction between transition metal (TM) solutes and hydrogen in the interstitial site as well as the vacancy in tungsten. We showed that the site preference of the hydrogen atom is significantly influenced by the solute atoms, which can be traced to the charge density perturbation in the vicinity of the solute atom. The solute-H interactions are mostly attractive except for Re, which can be well understood in terms of the competition between the chemical and elastic interactions. The chemical interaction dominates the solute-H interaction for the TM solutes with a large atomic volume and small electronegativity compared to tungsten, while the elastic interaction is primarily responsible for the solute-H interaction for the TM solutes with a small atomic volume and large electronegativity relative to tungsten. The presence of a hydrogen atom near the solute atom has a negative effect on the binding of other hydrogen atoms. The large positive binding energies among the solute, vacancy and hydrogen suggest that they would easily form a defect cluster in tungsten, where the solute-vacancy and vacancy-H interaction contribute greatly while the solute-H interaction contributes a little. Our result provides a sound theoretical explanation for recent experimental phenomena of hydrogen retention in the tungsten alloy and further recommends a suitable W–Re–Ta ternary alloy for possible plasma-facing materials (PFMs) including the consideration of the hydrogen retention.

Keywords: tungsten, hydrogen retention, solute-H interaction, first-principles calculations

(Some figures may appear in colour only in the online journal)

1. Introduction

Hydrogen in metals has been the subject of intensive research activities over the last few decades, motivated by the interest in basic scientific and technological applications, and by the problems posed by the material failure processes. Recently, the tungsten-hydrogen system has received particular attention because tungsten is considered the primary candidate for the plasma-facing material (PFM) of fusion reactors [1–3]. Fusion energy production relies on the reaction of the hydrogen isotopes deuterium (D) and tritium (T) forming helium and releasing 14 MeV neutrons. In the magnetic confinement approach for thermonuclear fusion, D–T plasmas at a temperature of around 15 keV (about 150 million K) are trapped in a toroidal magnetic field inside a vacuum vessel. Due to the imperfect confinement, the hydrogen isotopes escape from the plasma and interact with the vacuum vessel wall. This causes the hydrogen isotopes to become trapped in the wall material,

making it unavailable for fusion, and degrading the fuelling efficiency of the burning plasma. On the other hand, tritium is expensive and in short supply. Furthermore, a high retention of hydrogen isotopes in the PFM leads to the modification of the material's physical and mechanical properties, causing such effects as bubble formation, swelling, embrittlement, and surface roughening and blistering, and finally inducing the failure of the PFM. Thus, one of the key requirements of potential PFMs is low hydrogen retention.

As a potential candidate material, tungsten features a very low solubility for hydrogen among other favourable properties such as a low physical sputtering yield and a high melting temperature. However, a certain amount of hydrogen may still be permanently retained in tungsten due to the existence of the lattice crystal defects in the material [4]. The hydrogen atoms tend to concentrate at the lattice defect (e.g. dislocations, grain boundaries and voids) such that a high hydrogen concentration region forms. This region, acting as a start point, enables bubble and blister formation, which significantly degrades the mechanical properties of the materials. The hydrogen-induced failures correlate closely to the hydrogen diffusion and aggregation in the materials. Generally, hydrogen has high mobility in tungsten. The diffusion of hydrogen may be blocked by the lattice imperfections, such as point-defects and solute atoms. Due to their interaction with hydrogen, the lattice imperfections effectively increase the time to desorb a hydrogen atom from its lattice site and increase the apparent activation energy for diffusion. Therefore, the interactions of hydrogen with lattice imperfections dominate largely the hydrogen effective diffusivity and thereby the hydrogen retention.

The configurations and energetics of the interaction between the lattice imperfections and the hydrogen in metals, needed for the understanding of the hydrogen behaviour at an atomic scale, may be not easily accessible by experimental measurements. However, theoretical calculations or modelling methods can provide an indispensable way to explore the underlying physical mechanisms and compare them with experiments. Until now, a great amount of work has been done to investigate the interaction of hydrogen with point defects, including the vacancy and self-interstitial, in tungsten. Recently, Lu *et al* gave an effective review of this subject [5]. Besides vacancy and self-interstitial atoms, solute atoms are another source that affect the hydrogen solution and diffusion. The influence of solute atoms on the hydrogen solution and diffusion has been systematically investigated in metals such as Ti, Pd, etc [6–12]. However, similar investigation in tungsten is very limited. Up to now, the published binding energies in tungsten were only reported for a few solute elements (see [13] for a review of the subject), such as C [14–18], N [19], O [18], Re [20], and Os [20]. But in fact, the solute atoms in tungsten are diverse, which can be either voluntarily added to tailor the properties of a metal, or left out from the elaboration process. Furthermore, during its service in fusion reactors, tungsten and its solute atom will be transmuted to their near neighbours in the periodic table by the 14 MeV fusion neutrons, which makes the situation even more complicated [21]. Recently, a few experimental works have been performed to investigate the influence of solute atoms on the hydrogen retention in tungsten. These experiments clearly showed that the solute atoms can significantly change the hydrogen retention in tungsten [22–28]. Therefore, the study of solute-hydrogen (solute-H) interaction has an important role in the reliable predication of hydrogen recycling and retention in tungsten, particularly in its alloy.

Beyond the technological implications, the mechanism of the solute-H interaction in metals is also of scientific interest. The interaction of hydrogen with solutes in metals is mainly ascribed to two effects, i.e. the elastic interaction and the chemical interaction [29]. For the elastic interaction, the hydrogen atom is attractive to the undersized solute atom (i.e. the solute atom with a smaller atomic radius than the host atom) and repulsive to the oversized solute atoms since the lattice expansion induced by hydrogen is released by the tensile strain field near the undersized solute atom and further increased by the compressive strain field near the oversized solute atom [30]. On the other hand, a conflicting model has been suggested by Westlake and Miller, i.e. the oversized solute atom distends the nearby interstitial sites in such a way so as to accommodate the hydrogen atom more favourably [31, 32]. For the chemical interaction, the hydrogen tends to be trapped by the solute atoms with a higher chemical affinity for hydrogen than the host element. More specifically, the solute-H binding is dominated by the elastic interaction in the case of interstitial solutes [29]. For the transition metal (TM) solutes, there is a comparable contribution from both the elastic and chemical interactions, with the degree of attraction increasing with the size of the solute and its number of *d* electrons [29]. These models have successfully explained the solute-H interaction in metals, such as Fe [8, 9] and Ti [6], and have also been applied to the interaction between other interstitial atoms and substitutional solutes, such as O in Nb and V [33], and C in Fe [34]. However, there are still a lot of problems in the practical usage of these models. For example, these models fail to explain the interaction of the TM solutes with hydrogen in Nb [7]. The mechanism of the solute-H interactions is still an open question. Here, the question naturally arises as to what will happen in tungsten.

In our previous works [18, 19], we have performed a series of first-principles calculations to investigate the interaction between hydrogen atoms and the interstitial solute atoms. Here, we extend our research to the study of the interaction between hydrogen and substitute solute atoms. All the TM metal elements in the third, forth, and fifth periods (denoted by 3d, 4d, and 5d, respectively) of the periodic table are involved in the present study. Among which, some of the TM elements are alloyed in W to tailor the mechanical properties, such as Re, Ta, Ti, and V [35, 36]. Re and Os are also the primary neutron-induced transmutation products of W, and Hf is a transmutation product of W isotopes [21]. Some of the TM elements, such as Mo, Fe, Cu, Mn, Cr, and Ni, are impurities in W [37]. Other TM elements are also considered in order to gain insight into the fundamentals and general trends of the solute-H binding. Since there are two typical dissolution sites, i.e. the interstitial site and the vacancy, for hydrogen retention in tungsten, we systematically investigate the interaction structures and energetics between the solute and hydrogen

in the interstitial site and the vacancy, respectively, using first-principles calculations. And then, using these energetics parameters, we estimate the influence of some solute atoms on hydrogen dissolution and diffusion in tungsten. These results will not only be quite helpful to understand the solute-H interaction but can also provide a sound explanation for recent experimental phenomenon, and furthermore propose guidance for the design of the alloy composition in tungsten.

2. Computational method

The present calculations are performed within density functional theory as implemented in the Vienna *ab initio* simulation package [38, 39]. The interaction between ions and electrons is described by the projector-augmented wave method for different metals [40]. Exchange and correlation functions were taken in a form proposed by Perdew and Wang (PW91) within the generalised gradient approximation [41]. The supercell composed of 128 lattice sites ($4 \times 4 \times 4$ of the conventional body centered cubic cell) is used. The plane wave cutoff and k-point density are both checked for each system to achieve an energy convergence of 0.001 eV per atom for the electronic minimisation. Following a series of test calculations a plane wave cutoff of 500 eV is used and a k-point grid density of $3 \times 3 \times 3$ is employed. The relaxations of atomic position and optimisations of the shape and size of the supercell are performed. The structural optimisation is truncated when the forces converge to less than 0.001 eV Å^{-1}.

The hydrogen solution energy (S_{H}^{ς}) is defined as the energy needed for a hydrogen atom to move from the vacuum to the site ς in the bulk. In pure tungsten, it is expressed as

$$S_{\text{H}}^{\varsigma} = E_{\text{tot}}^{\text{H}} - (E_{\text{tot}}^{\text{bulk}} + 1/2E_{H_2}), \quad (1)$$

where $E_{\text{tot}}^{\text{H}}$ is the total energy of the supercell containing a single interstitial hydrogen, $E_{\text{tot}}^{\text{bulk}}$ is the total energy of perfect tungsten, and E_{H_2} is the energy of the H_2 molecule in the vacuum. Similarly, the hydrogen solution energy in the vicinity of the solute atom in tungsten can be calculated as follows

$$S_{\text{H}}^{\varsigma}(Sol) = E_{\text{tot}}^{Sol-H} - (E_{\text{tot}}^{Sol} + 1/2E_{H_2}), \quad (2)$$

where E_{tot}^{Sol-H} is the total energy of the supercell containing a solute-H pair ($Sol - H$), and E_{tot}^{Sol} is the total energy of the supercell with a substitutional solute atom.

The binding energies are used to evaluate the interactions between the defects (substitutional solute atom (Sol), vacancy (Vac), and interstitial hydrogen (H)). For the defect cluster containing two point defects (A_1, A_2), the binding energy is calculated as follows: [8]

$$E_b^{A_1,A_2} = E_{\text{tot}}^{A_1} + E_{\text{tot}}^{A_2} - E_{\text{tot}}^{A_1-A_2} - E_{\text{tot}}^{\text{bulk}}, \quad (3)$$

where $E_{\text{tot}}^{A_1}$ and $E_{\text{tot}}^{A_2}$ are the total energies of the supercell with A_1 and A_2, respectively, and $E_{\text{tot}}^{A_1-A_2}$ is the total energy of the supercell containing both A_1 and A_2. Here, the negative binding energy indicates repulsion between two point defects, while the positive binding energy means attraction.

For the defect cluster containing three point defects, two different binding energies are defined: [8] (i) the total binding energy, representing the stability of the cluster with respect to the isolated defects, defined as:

$$E_b^{A_1,A_2,A_3} = E_{\text{tot}}^{A_1} + E_{\text{tot}}^{A_2} + E_{\text{tot}}^{A_3} - E_{\text{tot}}^{A_1-A_2-A_3} - 2E_{\text{tot}}^{\text{bulk}}, \quad (4)$$

where $E_{\text{tot}}^{A_1-A_2-A_3}$ is the energy of the supercell with the defect cluster $A_1 - A_2 - A_3$, (ii) the incremental binding energy, defined as the energy difference between the supercell with a single point defect A_3 and a defect cluster $A_1 - A_2$ and the supercell with a defect cluster $A_1 - A_2 - A_3$,

$$E_b^{A_3,A_1-A_2} = E_{\text{tot}}^{A_1-A_2} + E_{\text{tot}}^{A_3} - E_{\text{tot}}^{A_1-A_2-A_3} - E_{\text{tot}}^{\text{bulk}}, \quad (5)$$

which is used to evaluate the synergistic effect between these effects.

3. Results

3.1. Site-occupation of the hydrogen atom

In body centered cubic tungsten, the TM solute atoms usually prefer to substitute tungsten atoms on the crystalline lattice site due to their large atom size. This has been confirmed by our previous works [42], where we found that the solution energies of the TM solutes in substitutional sites, ranging from −0.5 to 2.5 eV, are much lower than their corresponding solution energies in interstitial sites, ranging from 6 to 13 eV. For hydrogen, there are two possible interstitial sites in bcc tungsten, i.e. the tetrahedral interstitial site (TIS) and the octahedral interstitial site (OIS). The favourable interstitial position for the hydrogen atom is the TIS, where the solution energy is 0.93 eV, less than the value for the OIS, 1.31 eV. Our calculated results are in good agreement with the previously reported results [43–47]. It is interesting to consider whether the site preference of hydrogen changes or not when there is a substitutional solute atom nearby. To answer this question, the solution energies of hydrogen initially placed in the first nearest neighbour TIS or OIS of the solute atom are calculated. We note that, after geometric optimisation, the position of the hydrogen initially placed in the OIS does not change very much for all the solute atoms, whereas the hydrogen atom initially placed in the TIS may move significantly away from the perfect TIS for some of the solutes (we will come back to this point later in section 4). As shown in figure 1, the hydrogen solution energies in the TIS are mostly still less than those in the OIS with four exceptions (Mn, Fe, Co, and Ni), suggesting that the hydrogen still prefers the TIS over the OIS in the vicinity of the solute atom. For the solute atoms of Mn, Fe, Co, and Ni, the solution energies are very close for both interstitial sites, indicating that the site preference tendency disappears. We further calculated the hydrogen solution energies with the hydrogen atom in the second and third nearest neighbouring TIS and OIS of these four solutes. We found that the TIS is still more energetically favourable than the corresponding OIS. This is understandable since the influence of the solute diminishes with the increasing distance between H and the solute atom. Therefore, in the following, we only discuss the situation of the TIS hydrogen in the vicinity of a substitutional solute atom.

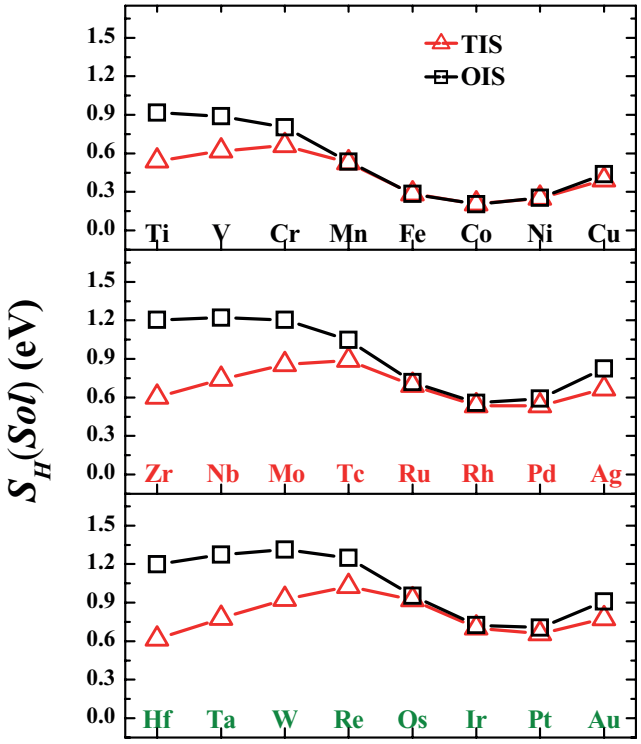

Figure 1. The solute energy of hydrogen in the first nearest neighbour TIS and OIS of the substitutional solute atom. The mark 'W' means the case in a pure tungsten material; it has the same meaning in the following figures unless otherwise specified.

3.2. Binding energies of the solute − H pair and sol − 2H clusters

For the solute-H interaction, the binding energy and the interaction radius are two important parameters, which can quantitatively characterise the strength and range of the interaction, respectively. Here, a model has been constructed to calculate these two parameters, where the solute atom substitutes a tungsten atom and the hydrogen is inserted in different neighbouring TISs of the solute atom. Figure 2 displays the binding energies of the solute with the hydrogen atom at its first to fourth nearest neighbour TISs (1nn to 4nn). The solute-H interaction decreases sharply with the increasing distance. The interaction is strong at the first and second nearest neighbour shells, and then becomes very weak at the third nearest neighbour distance, and finally vanishes for a larger separation distance. These results suggest that the solute-H interaction is very local; limited within the second nearest neighbour shell. Most of the solute-H binding energies are positive, suggesting an attractive interaction between the solute atom and hydrogen. The exceptions are Re–H and Os–H with negative binding energies, implying a repulsive interaction. However, the absolute values of the binding energies are so small (less than 0.03) that the repulsive interaction is negligible for the Os–H pairs. This is consistent with previous results [20]. In addition, it can be clearly seen from figure 2 that the solute-H interaction exhibits a similar wave-like trend with an increasing atomic number in each series of 3d, 4d, and 5d. For the 4d and 5d series, the solute-H interaction energy reaches the minimum and maximum at group 7 and 10 of the periodic

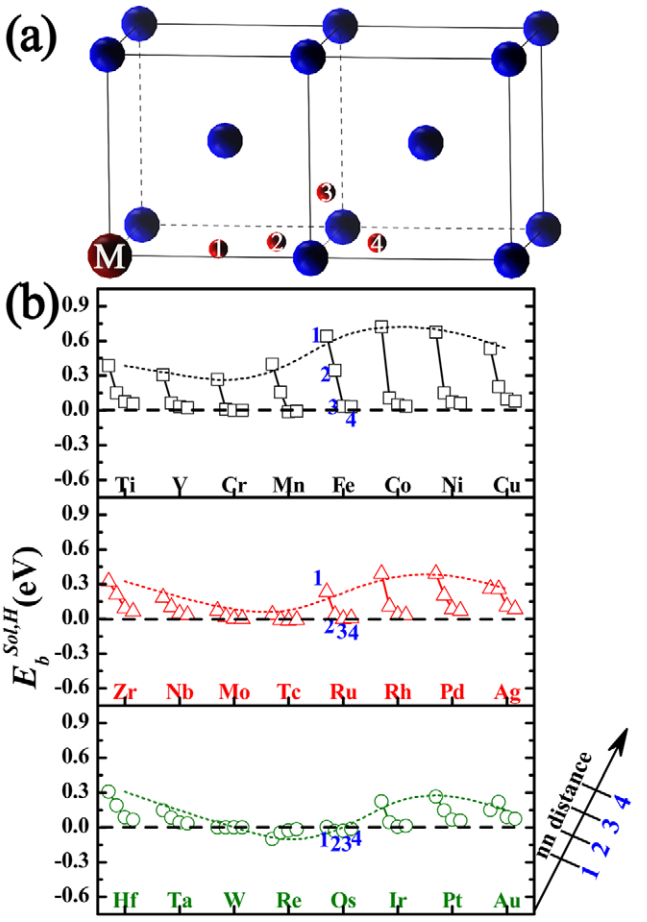

Figure 2. (*a*) The schematic diagram of *solute* − *H* pairs and (*b*) their corresponding binding energies. The tungsten and solute atoms are represented by the large blue and red balls, respectively. The solute atom is marked with 'M'. The interstitial sites at the first to fourth nearest neighbour shells of the solute atom are denoted by the small red balls, named by $1 \sim 4$ in turn, which are presented as the arrows in the right bottom region in (*b*). Take the case of Fe for example: the binding energies of Fe with a single hydrogen at its first to fourth nearest neighbour shells are read from left to right, marked by the '$1 \sim 4$', in turn. The dash lines are presented as guides for the eye for the solute-H binding energy at the first nearest neighbour shell. Note that, the sites 1–4 are just initial positions in the calculations of the structure relaxation. (For an interpretation of the references to colour in this figure legend, the reader is referred to the web version of this article).

table, respectively. There is a little difference for the 3d elements, where the solute-H interaction energy reaches the minimum at group 6 and the maximum at group 9. Note that the solute-H interactions are much stronger for the 3d elements than the corresponding 4d and 5d elements. Similar results have also been found in the interaction between TM solutes and helium [13, 48, 49].

It is well known that the interaction between interstitial hydrogen atoms is basically repulsive; self-trapping cannot make seeds for hydrogen bubbles [50–52]. This is also confirmed by our results. As shown in figures 3(*a*) and (*b*), the binding energy of the *H*−*H* pair decreases (in absolute value) rapidly with the increasing *H*−*H* distance, which almost vanishes for the configuration beyond 3. For the configurations 1 and 2, the binding energy is negative, implying a

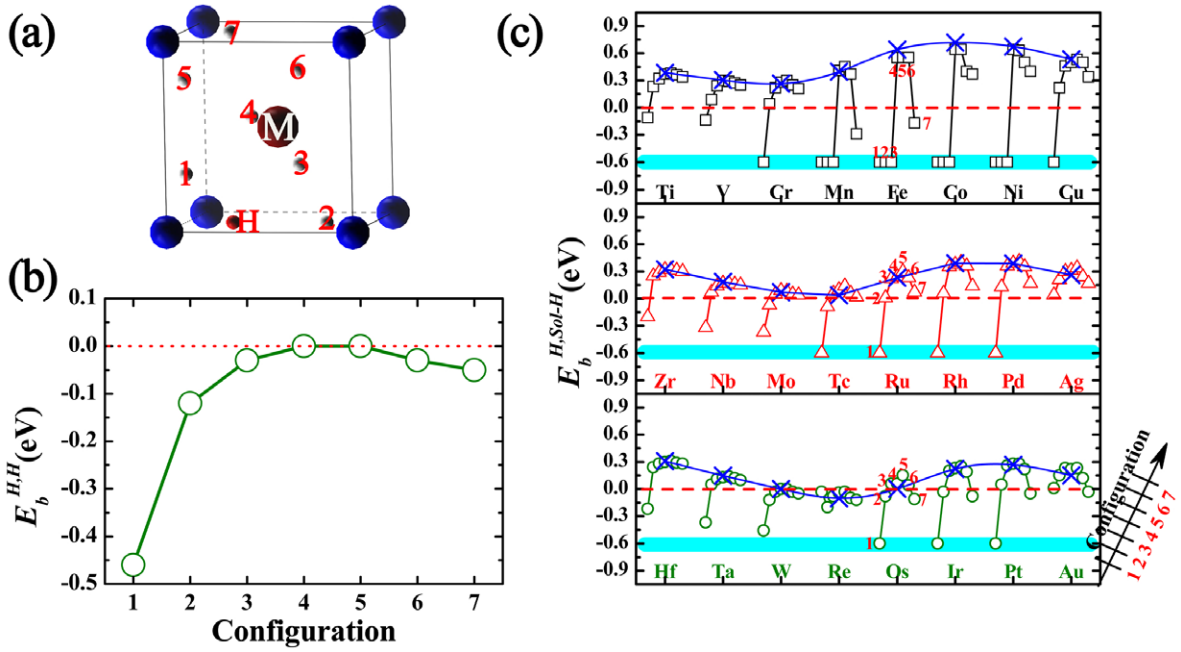

Figure 3. (*a*) The schematic diagram of two TIS hydrogen atoms in tungsten with and without a solute atom. In pure tungsten, the first hydrogen atom is placed on the site denoted by the small red ball, the second hydrogen occupies the site labelled with *i*, denoted by the small white ball. In the system with a solute atom, the TM solute atom substitutes the tungsten atom, denoted by the red balls and marked with 'M'. (*b*) The binding energy of the $H-H$ pair in pure tungsten, $E_b^{H,H}$. (*c*) The incremental binding energies of the second hydrogen with the $solute-H$ pair, $E_b^{H,Sol-H}$. The insert axis represents the $E_b^{H,Sol-H}$ values of the seven plausible geometries for hydrogen pairs around an solute atom. Take Fe for example, the $E_b^{H,Sol-H}$ values are read from left to right, marked by the red '$1\sim7$', in turn. Here, the binding energies of the solute atom with a single hydrogen are also shown for comparison, which are denoted by the blue '$\times$' with the solid blue line. Note that the sites 1–7 in (*a*) are just initial positions in the calculations of the structure relaxation. Some of them are unstable and would spontaneously relax to other configurations after the structure relaxations, whose incremental binding energies are set to −0.6 eV (the wide cyan line) in (*c*), such as, sites 1–3 of Fe and site 1 of Ru and Os. (For interpretation of the references to colour in this figure legend, the reader is referred to the web version of this article).

repulsive interaction between the $H-H$ pair. However, the non-damaging irradiation experiments have demonstrated that hydrogen clusters form in tungsten [53, 54]. Since there is strong attractive interaction between the solute atom and hydrogen, a crucial question arises of whether the solute atom could act as the nucleation point of a hydrogen bubble, i.e. the solute atom can trap multiple hydrogen atoms to form hydrogen clusters. Therefore, we further investigate the situation of two TIS hydrogen atoms around a substitutional solute atom, i.e. the $solute-2H$ clusters. We construct seven possible geometries for the $solute-2H$ clusters, where two hydrogen atoms are placed in different TISs in the first nearest neighbour shell of the solute atom (see figure 3(*a*)). The seven geometries are denoted by configuration Nos. 1–7 with increasing $H-H$ distance.

In figure 3(*c*), we present the incremental binding energy of the second hydrogen atom with the $solute-H$ pair ($E_b^{H,Sol-H}$) against the $H-H$ distance for all solute atoms. The incremental energy increases drastically with the $H-H$ distance, reaches a maximum for configuration 4 or 5, and then drops slightly with the further increasing $H-H$ distance. This trend of the $E_b^{H,Sol-H}$ with $H-H$ distance is similar to that of $E_b^{H,H}$ in pure tungsten, indicating that there is a large synergistic effect between the hydrogen atoms surrounding the solute atom. Particularly, for most solutes except for Ag and Au, the incremental energy for the shortest $H-H$ distance is negative, which is due to the strong repulsive interaction between the nearest neighbouring hydrogen atoms. The incremental binding energy increases since the interaction between the hydrogen atoms weakens with the increasing $H-H$ distance. The maximum incremental binding energy is close to the $solute-H$ pair binding energy for the fourth and fifth configuration because, in such a case, the $H-H$ interaction vanishes. The maximum incremental binding energy is positive for all the solutes except for Re, indicating that the solute atom (except for the Re–H one) could attract more than one hydrogen atom to form clusters, and, therefore, impede the hydrogen diffusion. While the size of the solute-H cluster may be small due to the synergistic effect between the hydrogen atoms near the solute atom and the local scope of solute-H interaction. Since the incremental energy for Re is negative for all $H-H$ distance, Re is not expected to influence the hydrogen transport in tungsten. It should be noted that, the nearest neighbouring hydrogen atoms are repulsive to each other, and the $H-H$ distance (about 1.54 Å) in the most stable $Sol-2H$ configuration is much larger than the bond length of the H_2 molecule (0.75 Å according to the present calculation). Therefore, the H_2 molecule may not form in W without large free volume. In addition, the first configuration would spontaneously relax to other configurations for solutes from group 6–10 of the periodic table except for Re, Ag, and Au, which

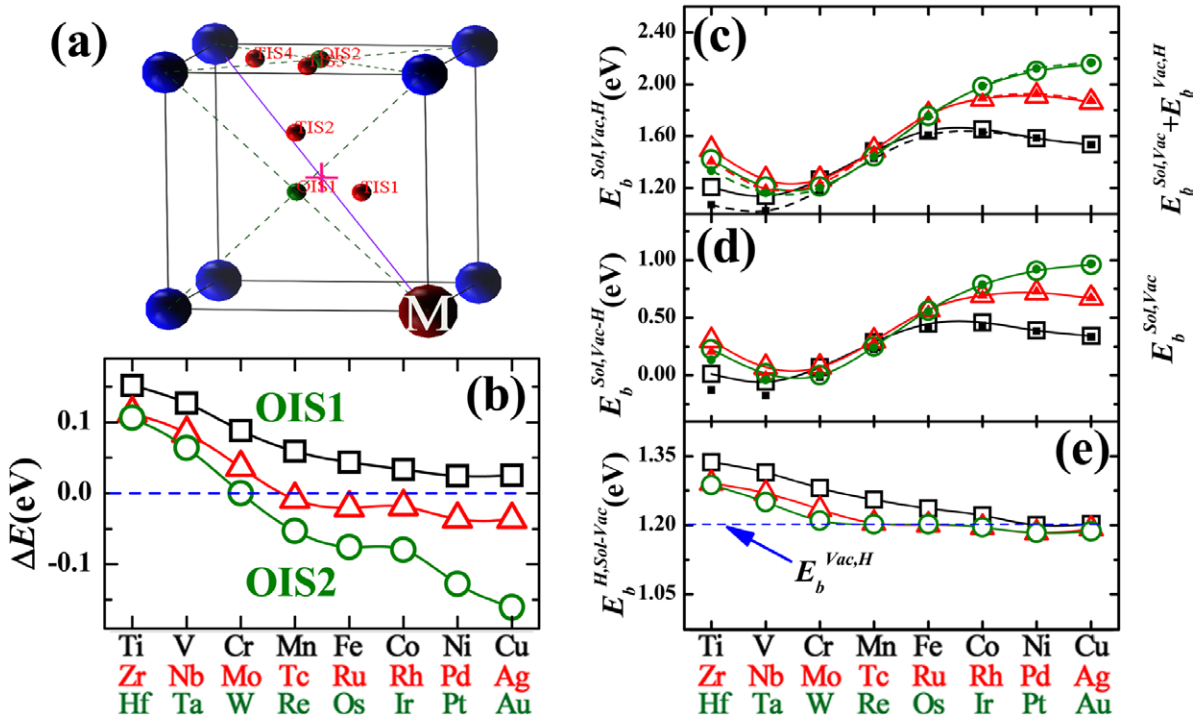

Figure 4. (*a*) The schematic diagram of the $Sol-Vac$ pair at the 1nn configuration (i.e. $<1\,1\,1>$ configuration) and six possible sites for hydrogen in the $Sol-Vac$ pair. The tungsten and the solute atoms are represented by the large blue and red balls, respectively. The six possible sites are denoted by the small balls. Among them, the red balls are for TIS1, TIS2, TIS3 and TIS4, and the green balls are for OIS1 and OIS2. (*b*) The energy difference when the hydrogen is located in OIS1 and OIS2, ΔE. (*c*) The total binding energies of the $Sol-Vac-H$ complexes, $E_b^{Sol,Vac,H}$, the sum of the binding energies of the $Vac-H$ pair and the binding energy of the $Sol-Vac$ pair, $E_b^{Vac,H}+E_b^{Sol,Vac}$, denoted by the hollow and solid icons, respectively. (*d*) The incremental binding energies between the solute atom and the $Vac-H$ pair, $E_b^{Sol-VacH}$, and the binding energies of the $Sol-Vac$ pair, $E_b^{Sol,Vac}$, denoted by the hollow and solid icons, respectively. (*e*) The incremental binding energies between the hydrogen and the $Sol-Vac$ pair, $E_b^{H-SolVac}$, and the binding energy of $E_b^{Vac,H}$ marked by the blue dash line. The black block, red triangle, and green circle represent the 3d, 4d, and 5d, respectively. (For an interpretation of the references to colour in this figure legend, the reader is referred to the web version of this article).

means that these solutes strengthen the repulsion between the nearest neighbouring hydrogen atoms.

3.3. Binding energy of the solute-vacancy-hydrogen (Sol − Vac − H) complex

Besides interstitial sites, the vacancy is also an important retention site for hydrogen in tungsten, especially in the case of irradiation, due to the large binding energy between the vacancy and hydrogen. For the case of a single hydrogen trapped in the vacancy, the most stable site for the H atom is a position ∼1.28 Å off the vacancy but close to the OIS, with a binding energy of ∼1.2 eV [5]. Here, this stable configuration is named by the vacancy-H ($Vac-H$) pair, $E_b^{Vac,H}=1.2$ eV. The vacancy may also attract TM solute atoms and form a stable solute-vacancy ($Sol-Vac$) pair, i.e. the TM solute atom occupies a substitutional site and a vacancy is in the nearest neighbouring sites of the TM solute. Our previous works [42] showed that the interaction of the $Sol-Vac$ pair at the first nearest neighbour shell is attractive and has the largest binding energy relative to other nearest neighbour shells for most TM solutes except for Ti and V (details can be found in [42]). Therefore, the solute atoms are expected to affect the hydrogen's behaviour in the vacancy. In this regard, the energetic of the $Sol-Vac-H$ is investigated. Based on the most stable configuration of the $Sol-Vac$ pair, we further incorporated a single hydrogen atom into the $Sol-Vac$ pair. Six different configurations are considered by taking into account the symmetry. Figure 4(*a*) shows the six possible sites for hydrogen in the $Sol-Vac$ pair, including four TISs (named TIS1, TIS2, TIS3, and TIS4, in turn) and two OISs (named OIS1 and OIS2, respectively). Note that although the Ti and V solute atoms do not thermodynamically bind with the vacancy in tungsten, the $Ti-Vac$ and $V-Vac$ at the 1nn configuration are also studied for data integrity. After full relaxation, the stablest configurations of $Sol-Vac-H$ are obtained. Similar to the pure tungsten system, the hydrogen atom finally relaxes to the position off the vacancy center but close to the OIS, i.e. the hydrogen atom initially in TIS1/TIS2 is relaxed to OIS1 and the one in TIS3/TIS4 is relaxed to OIS2 as shown in figure 4(*a*). The energy differences between the configurations with the hydrogen located in OIS1 and OIS2 are presented in figure 4(*b*). The site (OIS1) near the solute atom is more stable than the site (OIS2) away from the solute atom for all 3d and some early 4d and 5d elements, including Zr, Nb, Mo, Hf, and Ta, while the situation is opposite for the other solute elements.

Based on the stablest configuration of the $Sol-Vac-H$ complex, the total binding energies of the $Sol-Vac-H$ complexes ($E_b^{Sol,Vac,H}$) are calculated and summarised in figure 4(*c*). The total binding energies of the $Sol-Vac-H$ complexes are in the range of 1.20–2.20 eV. These large positive values indicate that the $Sol-Vac-H$ complexes are energetically favourable with respect to the isolated defects. It can thus be inferred that the solute, vacancy, and hydrogen would easily form a defect cluster in tungsten.

To explore the synergistic effect, the incremental binding energies between the solute atom and the $Vac-H$ pair ($E_b^{Sol,Vac-H}$) and that between hydrogen and the $Sol-Vac$ pair ($E_b^{H,Sol-Vac}$) are calculated based on the stable configuration of the $Sol-Vac-H$ complex (see figures 4(*c*) and (*d*)). For comparison, the binding energies of the $Sol-Vac$ ($E_b^{Sol,Vac}$) and $Vac-H$ pairs ($E_b^{Vac,H}$) are also shown in figures 4(*c*) and (*d*), respectively. It can be clearly seen that (i) the incremental binding energies of the solute atom with the $Vac-H$ pair, $E_b^{Sol,Vac-H}$, are similar to that with an individual vacancy, $E_b^{Sol,Vac}$; (ii) the incremental binding energies of hydrogen with the $Sol-Vac$ pair, $E_b^{H,Sol-Vac}$, are comparable to that with an individual vacancy, $E_b^{Vac,H}$, in all cases, despite the fact that the $Sol-H$ binding energies are very different for different solutes. These results suggest that the presence of the solute near the vacancy has little effect on the binding between the vacancy and the hydrogen in the vacancy also has little effect on the solute-vacancy interaction. Therefore, it can be concluded that the solute–H interaction plays a minor role in the $Sol-Vac-H$ complex, where the $Sol-Vac$ and $Vac-H$ interactions dominate. This is further confirmed by the results that the vast majority of the values of the total binding energies $E_b^{Sol,Vac,H}$ are equal to the sum of the binding energies of the $Vac-H$ pair, $E_b^{Vac,H}$, and the binding energy of the $Sol-Vac$ pair, $E_b^{Sol,Vac}$, i.e. $E_b^{Sol,Vac,H} \approx E_b^{Vac,H} + E_b^{Sol,Vac}$. Similar results have been found in Fe and have been suggested to support the hydrogen-enhanced stress-induced vacancy mechanism, in which Vac-H interactions play a significant role in hydrogen embrittlement [8]. In addition, it should be noted that the incremental binding energies of hydrogen with the $Sol-Vac$ pair are slightly larger than that with the vacancy in the case of all 3d and some early 4d and 5d elements, including Zr, Nb, Mo, Hf, and Ta. This suggests that the presence of these solute atoms marginally enhances the ability of a vacancy binding the hydrogen atom.

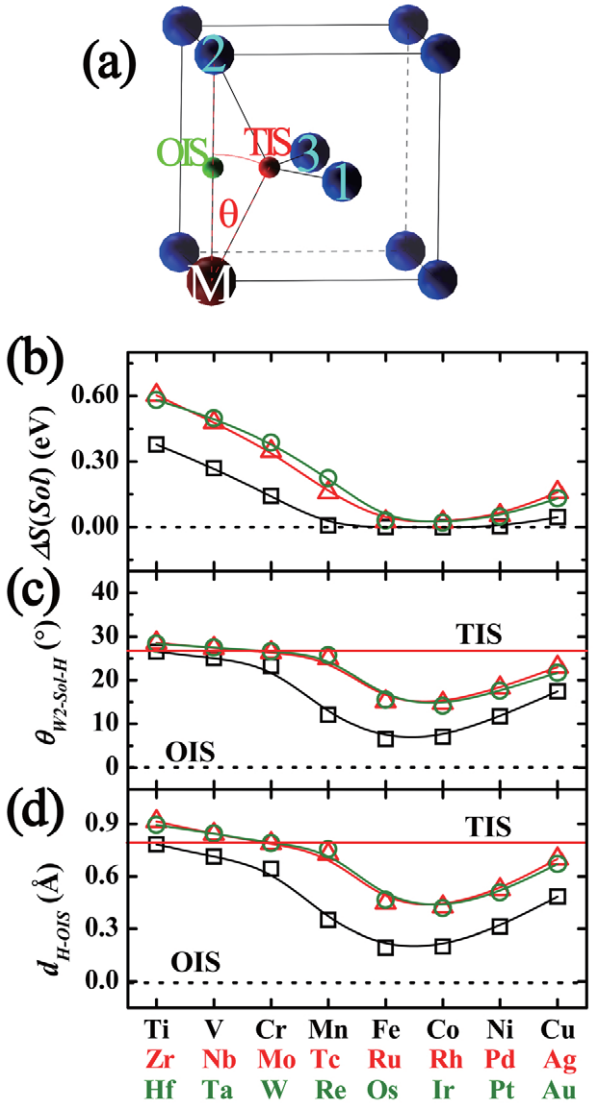

Figure 5. (*a*) The interstitial sites near the solute atom. The lattice site in bcc tungsten is denoted by the large blue and red balls. In the system with the solute, the solute atom is located in the site 'M' (the large red ball). The solute atom and three tungsten atoms, located in sites 1, 2, and 3, make up a tetrahedron. The TIS and OIS are denoted by the small red and green balls, respectively. (*b*) The solution energy difference between hydrogen in the TIS and OIS, $\Delta S(Sol)$. (*c*) The angle formed by the hydrogen atom, the solute atom, and the neighbouring tungsten atom, $\theta_{W2-Sol-H}$. (*d*) The distance between the hydrogen atom and the OIS for the optimised supercells with the hydrogen atom initially in the TIS, $d_{\mathrm{H-OIS}}$. The red solid and black dash lines represent the values when the hydrogen atom occupies the TIS and OIS in pure tungsten, respectively. The black block, red triangle, and green circle represent the 3d, 4d, and 5d, respectively. (For interpretation of the references to colour in this figure legend, the reader is referred to the web version of this article).

4. Discussion

4.1. Physics underlying the site occupation of hydrogen in tungsten alloys

According to the results of section 3.1, we know that the behaviour of the hydrogen site preference changes when there is a substitutional solute atom nearby. Here, we discuss its underline physics. For the sake of conciseness, the site preference of the TIS over the OIS are characterised by the solution energy difference of hydrogen in the TIS and the OIS ($\Delta S = S_{\mathrm{H}}^{\mathrm{TIS}} - S_{\mathrm{H}}^{\mathrm{OIS}}$ and $\Delta S(Sol) = S_{\mathrm{H}}^{\mathrm{TIS}}(Sol) - S_{\mathrm{H}}^{\mathrm{OIS}}(Sol)$ for the system without and with the solute atom, respectively, named by the site preference energy.). As shown in figure 5(*a*), for the solutes in the same group of the periodic table, $\Delta S(Sol)$ is almost the same for the solutes in the 4d and 5d periods whereas the 3d one is smaller. For the solutes in the

same period of the periodic table, with an increasing number of d electrons, the site preference energy $\Delta S(Sol)$ decreases for the early TM solutes in the periodic table (from Ti to Mn, Zr to Tc, and Hf to Re for the 3d, 4d, 5d periods, respectively), reaches the minimum (about zero) for the TM metal solutes (Fe/Ru/Os and Co/Rh/Ir), and then increases for the later ones. Comparing ΔS and $\Delta S(Sol)$, we see that the solute with d electrons less than tungsten enhances whereas those with d electrons more than tungsten weakens the site preference of the hydrogen atom in the TIS over the OIS. The site preference diminishes for the middle TM solute.

To understand the trend of the site preference energy against the solute atoms, we turn to analyse the geometric configuration of the solute-H pair. Figures 5(c) and (d) present the angle $\theta_{W2-Sol-H}$ formed by the hydrogen atom, the solute atom, and the neighbouring tungsten atom, and the distance $d_{\mathrm{H-OIS}}$ between the hydrogen atom and the OIS for the optimised supercells with the hydrogen atom initially in the TIS, respectively. For the hydrogen atom in the perfect TIS, $\theta_{W2-Sol-H}$ and $d_{\mathrm{H-OIS}}$ are about 26.7 degrees and 0.794 Å (1/4 lattice constant), respectively. For the hydrogen in the perfect OIS, both $\theta_{W2-Sol-H}$ and $d_{\mathrm{H-OIS}}$ are zero. It is seen that, for the early TM solutes before tungsten, both $\theta_{W2-Sol-H}$ and $d_{\mathrm{H-OIS}}$ are close to the values (26.7 degrees and 0.794 Å) for the perfect TIS indicating the hydrogen atom is still in the TIS near these solutes. With an increasing number of d electrons of solute, $\theta_{W2-Sol-H}$ and $d_{\mathrm{H-OIS}}$ decrease, indicating that hydrogen is pulled gradually from the TIS to the OIS. However, both $\theta_{W2-Sol-H}$ and $d_{\mathrm{H-OIS}}$ may not reach 0, such that the hydrogen atom may not enter the 'perfect' OIS but stop in-between the TIS and the OIS. For the later TM solute, hydrogen goes back to the TIS gradually with an increasing number of d electrons. The site preference energy $\Delta S(Sol)$ correlates closely to $\theta_{W2-Sol-H}$ and $d_{\mathrm{H-OIS}}$, i.e. $\Delta S(Sol)$ decreases with the hydrogen approaching the OIS.

To understand the physics of the site preference of hydrogen in tungsten alloys, we plot the charge density of the tungsten alloys in figure 6. For perfect tungsten, the charge density shows a perfectly regular waveform along the line of OIS-TIS-OIS-TIS-OIS with a trough at the OIS and a peak at the TIS. Such a regular trend is disturbed by the solute atoms. Let us take 5d solutes as an example: the peak at $\mathrm{TIS_1}$ moves away from the $\mathrm{OIS_1}$ for Hf and Ta, locating in-between $\mathrm{TIS_1}$ and $\mathrm{OIS_2}$, but shifts toward to $\mathrm{OIS_1}$ and stops in-between $\mathrm{TIS_1}$ and $\mathrm{OIS_1}$ for Re and Os. For Ir and Pt, the peak at $\mathrm{TIS_1}$ almost disappears and becomes a platform, whereas for Au, a very small peak re-appears in-between $\mathrm{TIS_1}$ and $\mathrm{OIS_1}$. It is more interesting that, with the increasing number of d electrons, the distance between the peak position and $\mathrm{OIS_1}$ decreases for the early TM solutes and reaches the minimum (i.e. disappears) for the middle TM solutes, and then increases for the later ones. Similar results can also be found in 4d. For the 3d, the peak at $\mathrm{TIS_1}$ moves away from the $\mathrm{OIS_1}$ for Ti, V, Cr, and Mn, and disappears for Fe, Co, Ni, and Cu. The correlation between the charge density and the site preference suggests that the charge density perturbation give rise to the changes of the site preference in the vicinity of the solute atom.

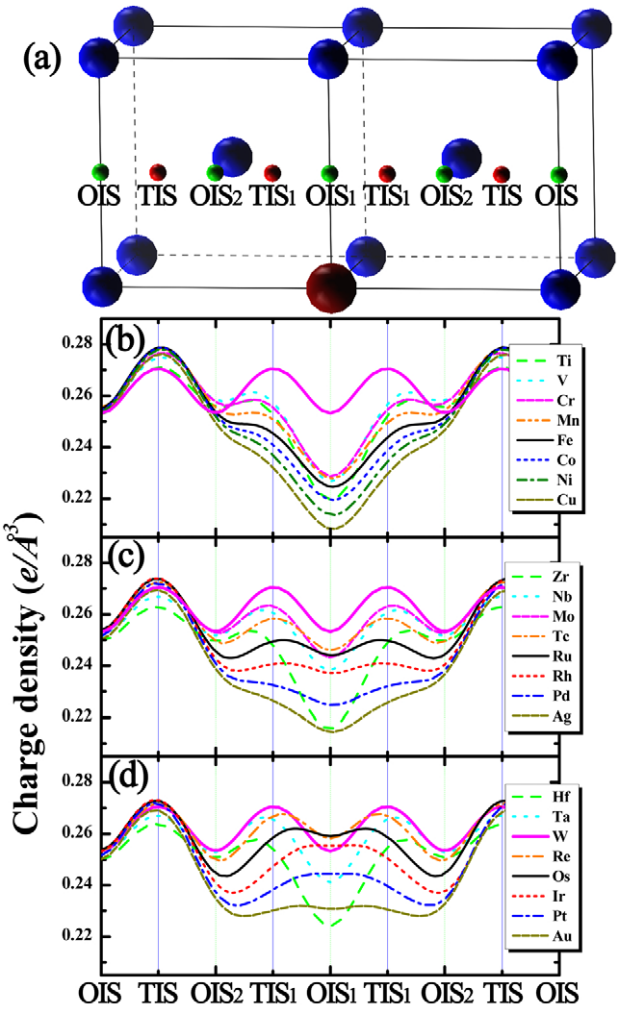

Figure 6. (a) The schematic diagram of the line of OIS-TIS-OIS-TIS-OIS of the tungsten system with and without solute atoms. The lattice site is denoted by the large ball. The solute atom is located in the site denoted by the large red ball and marked with 'M'. The TIS and OIS sites are denoted by the red and blue small balls, respectively. (b)–(d) Present the electron density distribution along the line of OIS-TIS-OIS-TIS-OIS of the tungsten system with and without 3d, 4d, and 5d TM solute atoms, respectively. The magenta solid line represents the result in pure tungsten. (For an interpretation of the references to colour in this figure legend, the reader is referred to the web version of this article).

4.2. Physics controlling the solute-H interaction

The solute-H interaction was attributable mainly to both the elastic and chemical interactions. For the elastic interaction, the solute size is a salient physical factor. Figure 7(a) gives the solute atomic volume Ω, extracted from [55]. Only Ti, Zr, Hf, Nb, Ta, Ag, and Au have the larger atomic volume than tungsten, namely, they are oversized solute atoms. The other elements have a smaller atomic volume than tungsten, i.e. they are undersized solute atoms. Furthermore, the 3d elements have much larger atomic volume differences to tungsten than most of 4d and 5d, suggesting that the elastic interaction would play a much bigger role in the interaction of 3d-H than 4d and 5d-H. Also plotted in figure 7(a) is the

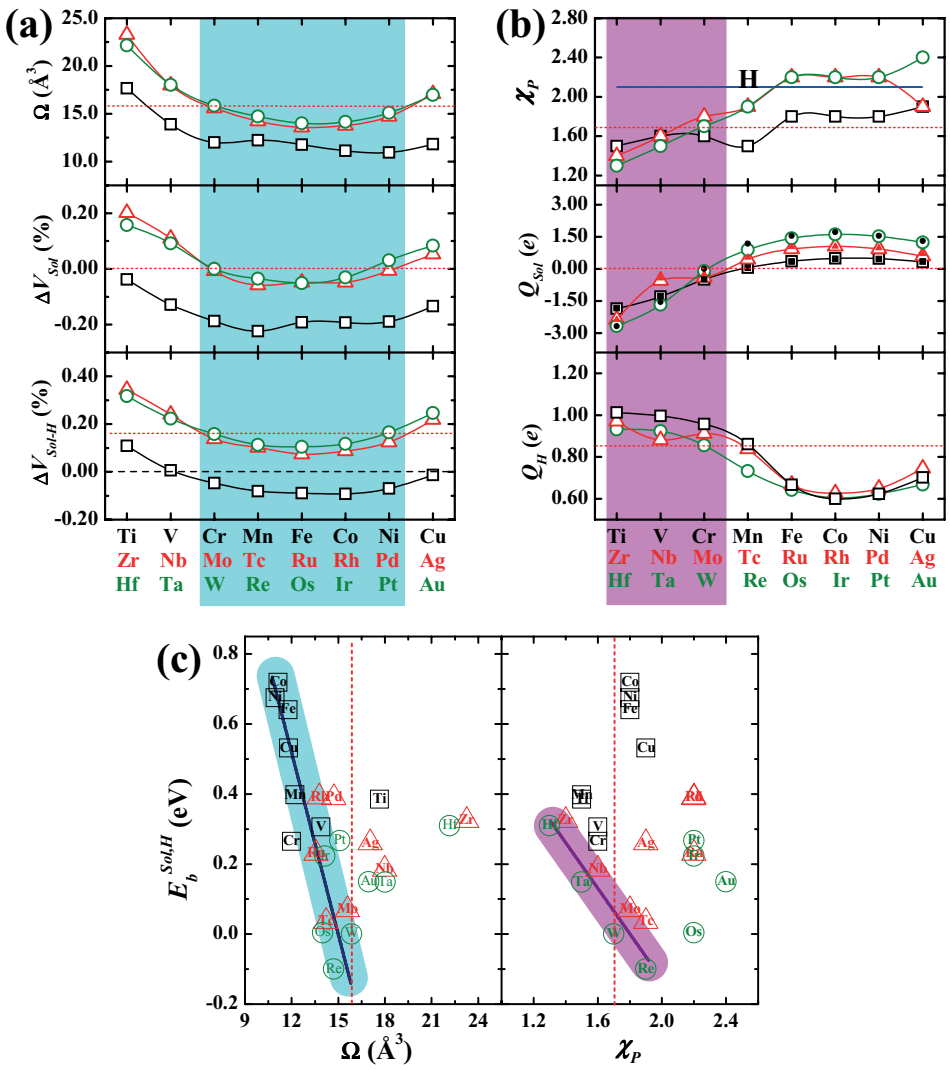

Figure 7. (*a*) The solute atomic volume Ω, extracted from [55], and the volume change of the supercell caused by the solutes, ΔV_{Sol}, and the solute-H pair, ΔV_{Sol-H}. (*b*) The electronegativity of the solute elements and hydrogen, χ_P, and the Bader charge of the solute, Q_{Sol}, and the hydrogen, Q_{Sol}. (*c*) The relation of the binding energy with the atomic volume and the electronegativity. The red dot line denotes the values of these physical quantities in pure tungsten. The blue line indicates the electronegativity of the hydrogen. In the case of the Q_{Sol}, the hollow and solid icons correspond to the situation of the solute atom with and without hydrogen nearby, respectively. (For an interpretation of the references to colour in this figure legend, the reader is referred to the web version of this article).

volume change of the supercell caused by the solutes, ΔV_{Sol}, which is given by subtracting the equilibrium system volume of pure solvent metal (V_W) from the equilibrium volume of the system with one solute (V_{Sol}) and then dividing by V_W, i.e. $\Delta V_{Sol} = (V_{Sol} - V_W)/V_W$. As seen from figure 7(*a*), the volume change follows remarkably the atomic volume trend, exhibiting a parabolic behaviour with the atomic number increasing in each serial of 3d, 4d, and 5d metals. Similar behaviours of the volume change caused by substitutional solutes have been observed in some other metals, such as Ti [6] and Fe [56]. Generally, the undersized solute atom reduces the equilibrium volume of the solvent metal, whereas the oversized atom increases it. Namely, the undersized and oversized solute atom shrinks and dilates the host lattice, respectively. In the case of interstitial hydrogen, the TIS hydrogen expands the equilibrium volume of the supercell about 0.16%. Note that this value applies only for the supercell used in this work, which would be lower with larger supercells. Therefore, one may expect that an undersized (oversized) solute atom releases (increases) the strain field induced by the hydrogen atom. This is true when we examine the volume change of the supercell induced by the $Sol - H$ pair, which is calculated as $\Delta V_{Sol-H} = (V_{Sol-H} - V_W)/V_W$, where V_{Sol-H} is the volume of the supercell containing a solute-H pair. Here, the data of the $Sol - H$ pair at the first nearest neighbour shell are used since they have the largest binding energy and are primarily responsible for the solute-H interaction. As seen from figure 7(*a*), the lattice expansion induced by the hydrogen is reduced in the presence of the undersized solute atom and increased by the oversized solute atom. Thus, according to the previous elastic interaction mechanism, it can be expected that there is an attractive interaction between the hydrogen and the undersized solute atom and a repulsive interaction between the hydrogen and the oversized solute atom. These results correspond well

Table 1. The distance between the solute atom and its nearby tungsten atoms relative to that in pure tungsten, Δd.

	Δd_{Sol-W1}	Δd_{W1-W2}	Δd_{Sol-W2}	Δd_{W1-W3}	ΔV_{TIS}
Ti	0.15	−0.15	−0.28	0.19	−14.05
Zr	1.67	0.91	0.57	1.70	−17.52
Hf	1.53	0.69	0.31	1.57	−18.20
V	−0.76	−0.55	−0.41	−0.76	2.35
Nb	0.69	0.40	0.28	0.72	−5.34
Ta	0.65	0.29	0.16	0.66	−6.83
Cu	0.33	−0.76	−1.32	0.35	18.09
Ag	1.82	0.04	−0.85	1.83	1.56
Au	2.11	0.15	−0.88	2.11	3.94

Note: For example, $\Delta d_{Sol-W1} = (d_{Sol-W1} - d_{W_{1\mathrm{nn}}})/d_{W_{1\mathrm{nn}}}$, $\Delta d_{Sol-W2} = (d_{Sol-W2} - d_{W_{2\mathrm{nn}}})/d_{W_{2\mathrm{nn}}}$. Here, $W_{1\mathrm{nn}}$ and $W_{2\mathrm{nn}}$ are the distance between a tungsten atom and its first and second nearest neighbour tungsten atom in pure tungsten, respectively. ΔV_{TIS} is the volume changes of the first nearest neighbouring TIS induced by the solute atom relative to that in pure tungsten. The corresponding configuration of the TIS is shown in figure 5 and nearest neighbouring tungsten atoms are indicated by 1–3. (in unit %).

with the positive binding energies of hydrogen with the undersized solute atom presented in figure 3 but contrary to that of the oversized solute atom.

Westlake and Miller have suggested that the oversized solute atom distends nearby interstitial sites in such a way that certain sites may become more favourable for hydrogen occupancy [31, 32]. It is indeed true that the distance between the oversized solute atom and its nearby tungsten atoms increases (see table 1). However, this does not mean that the volume of the nearby interstitial site is dilated. Due to its larger atomic volume, the solute atom would counteract the volume expansion resulting from the increase of the distance and even reduce the nearby interstitial sites. Therefore, the volume changes of the TIS induced by the solute atom (ΔV_{TIS}), including all oversized solute atoms and two undersized solute atoms V and Cu for comparison, have been calculated based on the hard-sphere model. The calculation procedure is as follows: the four atoms making up the tetrahedron are considered as the hard sphere with fixed radii, which are four tungsten atoms in the pure system and one solute atom and three tungsten atoms in the system with solute (see figure 5(*a*)). Then a new hard sphere is located into the tetrahedron and made to tangent to the four hard spheres by changing its center and radius. The center of this new hard sphere is defined as the tetrahedron interstitial site, and its volume is defined as the volume of the tetrahedron interstitial. In the pure tungsten lattice, the volume of the TIS, V_{TIS}, can be simply calculated by the analytic geometry, while in the system with the solute atom, the TIS volume, $V_{\mathrm{TIS}}(Sol)$, can be numerically solved by the simulated annealing algorithm. Thus, $\Delta V_{\mathrm{TIS}} = (V_{\mathrm{TIS}}(Sol) - V_{\mathrm{TIS}})/V_{\mathrm{TIS}}$. As presented in table 1, Ag and Au dilate the nearby TIS, supporting the Westlake and Miller model, whereas Ti, Zr, Hf, Nb, Ta compress the nearby TIS, apparently, whose interaction with hydrogen cannot be explained by the Westlake and Miller model. Furthermore, comparing figures 2 and 7(*a*), the trend of the solute-H binding energy across the 3d, 4d, and 5d row elements is different from that of the atomic volume and the volume changes, respectively, induced by the solute and the solute-H pair. Therefore, the solute-H interaction cannot be explained satisfactorily by the elastic interaction mechanism.

Apart from the elastic interaction, the chemical interaction is another important factor that influences the solute-H interaction. As far as the chemical interaction is concerned, it is easy to understand that the solute elements with higher affinity for hydrogen than the host tungsten will be attractive to hydrogen, and vice versa. However, it is difficult to find a quantitative measure for the solute-H affinity. According to the previous studies on the solute-H interaction [7, 8], the electronegativity may provide good approximations. Figure 7(*b*) shows the electronegativity of the solute elements and hydrogen. Compared to tungsten, the early elements, such as Ti, Zr, Hf, V, Nb, Ta, Cr, Mn, have a large difference in electronegativity with hydrogen, whereas other elements have a small difference. Therefore, the chemical affinity of the early elements with hydrogen is stronger than tungsten, suggesting an attractive interaction with hydrogen, and that of the others is weaker than tungsten, implying a repulsive interaction. Particularly, for 3d elements, the electronegative are very similar to tungsten, meaning a very weaker role for the chemical interaction in the solute-H interaction. These deductions can be further verified by the charge transfer since the difference in electronegativity drives the electron transfer. We further calculate the charge transfer induced by the solute and the solute-H pair, according to Bader charge analysis. Here, the Bader charges are calculated using a grid based on the algorithm developed by Henkelman *et al* [57, 58]. Figure 7(*b*) presents the Bader charge of the solute and the hydrogen. For the solute atom, the correlation between the electronegativity and the Bader charge is always straightforward. The early elements with small electronegativity lose electrons and become positively charged, while the later elements with large electronegativity gain the electron and become negatively charged. The Bader charge of hydrogen is 0.8 *e*, indicating the negatively charged hydrogen in tungsten. Thus, the early elements and the hydrogen with different charges attract each other, while the other elements and the hydrogen with the same charges repel each other. These results are in agreement with the binding energies of the early elements with the hydrogen but contrary to that of the latter elements. In addition, it should be pointed out that the presence of hydrogen has little effect on the Bader charge of the solute atom while the solute significantly influences the Bader charge of the nearby hydrogen.

As we discussed above, both the elastic and chemical interactions cannot independently explain satisfactorily the solute-H interaction obtained in the current work. There is an obvious competitive relationship between these two factors. For the early elements, the larger atomic volume suggests a repulsive interaction with hydrogen, disagreeing with the binding energy results, and the smaller electronegativity indicates an attractive interaction with hydrogen, as consistent with the binding energy results, whereas it is the contrary for the latter elements. Thus, it can be concluded that the elastic interaction is primarily responsible for the solute-H interaction in the case of the early elements (with small atomic volume and big electronegativity) and the chemical interaction dominates the solute-H interaction for the later elements

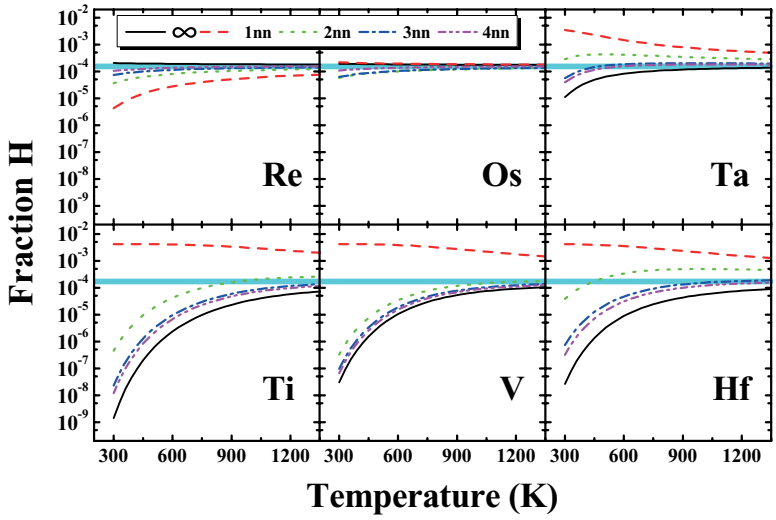

Figure 8. Hydrogen fraction in TISs around the solute atom for the first four shells (labelled with $1 \sim 4$ nn) around the solute atom and beyond (labelled with ∞) for a given concentration of the solute and hydrogen (10^{-2} and 10^{-3}, respectively) as a function of temperature. The blue line represents the fraction of hydrogen in the TIS in the pure tungsten. (For an interpretation of the references to colour in this figure legend, the reader is referred to the web version of this article).

(with big atomic volume and small electronegativity). These results can be clearly presented when we plot the relation of the binding energy with the atomic volume and the electronegativity. As can be seen in figure 7(*c*), the $Sol - H$ binding energies clearly show a negative correlation to the atomic volume for the latter elements and exhibit a negative correlation to electronegativity for the early elements.

4.3. Alloying elements in tungsten under a fusion environment

As mentioned in the section 1, tungsten is suggested to be used as the divertor plate in ITER. One problem associated with the technological applications of tungsten is its high ductile-to-brittle transition temperature [59, 60]. To improve the material's ductility, the alloying of tungsten with some ductile components has been proposed and thus stimulated extensive investigations. Besides the ductility, the influence of alloying additions on the retention of hydrogen isotopes in tungsten is also an important issue needing to be evaluated with the selection of alloying elements because the low hydrogen retention is one of the key advantages of tungsten as a potential plasma-facing candidate material. In the following discussion, we focus on the effects of some potential alloying elements, including Re, Ta, Ti and V, on hydrogen retention in material. Os and Hf, as the primary transmutation products of Re and W isotopes, respectively, are also discussed.

It is well accepted that hydrogen will redistribute in the material when some alloying elements are added. Recently, Simonovic *et al* [61] have proposed a model to quantitatively evaluate the effects of substitutional solutes on the distribution of interstitial solute atoms, when the interaction between substitutional solute atoms (SSA-SSA interaction) and the interaction between interstitial solute atoms (ISA-ISA interaction) can be neglected, and the ISA atoms diffuse much faster than the SSA atoms and arrange themselves around the SSA. The probability $f_{\rm inn}$ that an ISA is present at the ith nearest neighbouring cell of the SSA can be expressed as $f_{\rm inn} = f_\infty \exp[E_b^{\rm SSA-ISA}({\rm inn})/(k_{\rm B}T)]$. f_∞ is assumed to be a constant, representing the fraction of the interstitial sites filled with ISA where the SSA has no influence on the ISA. $E_b^{\rm SSA-ISA}({\rm inn})$ is the binding energy of the SSA with ISA at its ith nearest neighbouring shells. $k_{\rm B}$ and T represent the Boltzmann constant and the absolute temperature, respectively. Thus, assuming the SSA concentration relative to the lattice positions is $C_{\rm SSA}$, the ISA concentration $C_{\rm ISA}$ can be written as $C_{\rm ISA} = C_{\rm SSA}\sum_{i=1}^{\rm max} n_i f_{\rm inn} + \left(N_{\rm int} - C_{\rm SSA}\sum_{i=1}^{\rm max} n_i\right)$, where the n_i is the number of the interstitial sites on the ith nearest neighbouring shell of the SSA, and the $N_{\rm int}$ is the number of the interstitial sites per atom in the lattice. Combining the above two equations, it is easy to calculate the $f_{\rm inn}$ and f_∞ when the material composition is fixed. Particularly, without the solute atom, the f_∞ is given as $f_\infty = C_{\rm ISA}/N_{\rm int}$. The detailed calculation procedure can be found in [61].

Our previous work shows that the repulsive interactions between the alloying atoms cause them to move far apart from each other and form a random solid solution in tungsten [42]. The active energy of the hydrogen migration ($\sim$0.2 eV) is much smaller than that of the alloying atoms ($\sim$5.0 eV) indicating that the hydrogen diffuses much faster than the alloying atom [42, 62]. The former results on the solute-H interaction suggest that hydrogen can be arranged around the solute atoms to form interstitial hydrogen clusters. Therefore, it is reasonable to use Simonovic's model to investigate the effects of alloying elements on the distribution of hydrogen. Utilising the obtained $Sol - H$ binding energies, $f_{\rm inn}$ and f_∞ are calculated at a given concentration of the alloying element and hydrogen, i.e. $C_{Sol} = 10^{-2}$ and $C_{\rm H} = 10^{-3}$, respectively. In the case of the hydrogen dissolution in the TIS, the $N_{\rm int}$ is equal to 6, and the n_i is equal to 24, 24, 48, and 72 for $i = 1$, 2, 3, and 4, respectively. Thus, without the alloying addition, the fraction of hydrogen in tungsten is 1.67×10^{-4}. It can be clearly seen from figure 8 that the hydrogen fraction is slightly

repelled from the neighbour shells around Re and Os and is strongly drawn to the neighbour shells around Ta, Ti, V, and Hf, indicating that the hydrogen atoms can hardly be found in the neighbour shells nearby Re and Os but easily accumulate in the neighbour shells around Ta, Ti, V, and Hf, particularly in the 1nn shells. According to Simonovic's model, the chemical potential of the ISA is positively correlated with the fraction far away from the SSA. The SSA decrease the f_∞, and thus lower the ISA chemical potential, meaning the SSA increase the solubility of ISA in material. As can be seen in figure 8, the hydrogen fractions f_∞ for the Re and Os addition is similar to that for pure tungsten, whereas it is larger for the Ta, Ti, V, and Hf addition. Therefore, it can be expected that Re and Os have little effect on the hydrogen distribution while the segregation of hydrogen around Ta, Ti, V, and Hf increases the solubility of hydrogen in tungsten. It can also be seen that, with the temperature increase, the hydrogen fractions f_∞ for Ta, Ti, V, and Hf increases and gradually reaches the f_∞ value in pure tungsten. This indicates that the influence of Ta, Ti, V, and Hf on the hydrogen solubility in tungsten is a step-down with increasing temperature. Particularly, the effects of Ta may vanish above 700 K since the hydrogen f_∞ is similar to that in the pure tungsten at this temperature range.

Besides the distribution, the alloying elements also have consequences on the hydrogen diffusivity. Commonly, according to the classic Mac-Nabb and Forester formula, [63] the effective diffusivity of hydrogen in the solid solution can be simply described by

$$D_{\text{eff}} = \frac{D_{\text{perf}}}{1 + \frac{N_{Sol}}{N_{\text{W}}} \exp\left(\frac{E_b^{Sol-H}}{kT}\right)}, \tag{6}$$

where D_{perf} is the diffusivity at the perfect system without traps. Here, the diffusivity data, predicted in our previous work [62], is used as the diffusivity at the perfect system, which shows good agreement with the experimental data. C_{Sol} is the concentration of the solute, which is still set to be 10^{-2}. As shown in figure 9, Re and Os exert little effect on the hydrogen effective diffusivity, and Ta slightly decreases the hydrogen effective diffusivity, while Ti, V, Hf significantly reduce the hydrogen effective diffusivity. In addition, similarly to the case of distribution, the influence of Ta, Ti, V, and Hf on the hydrogen solubility in tungsten is a step-down with temperature increasing.

On the whole, Re and Os exert little effect on the hydrogen distribution and effective diffusivity. Ta, Ti, V, and Hf can trap multiple hydrogen atoms in their neighbour shells to form many small hydrogen clusters and decrease the hydrogen effective diffusivity, which could, to some extent, prevent the occurrence of large bubbles, but unfortunately would significantly increase the hydrogen retention in tungsten. The sequence of the solute effect is Os < Re < Ta $\ll$ V < Hf < Ti. It should be pointed out that the above conclusions about the influence of these solutes on the hydrogen retention are drawn only for the case without taking into account the effects of solute atoms on vacancies, which are considered as the predominant trapping sites for hydrogen under irradiation conditions. According to the former results in section 3.3, the presence of these solute

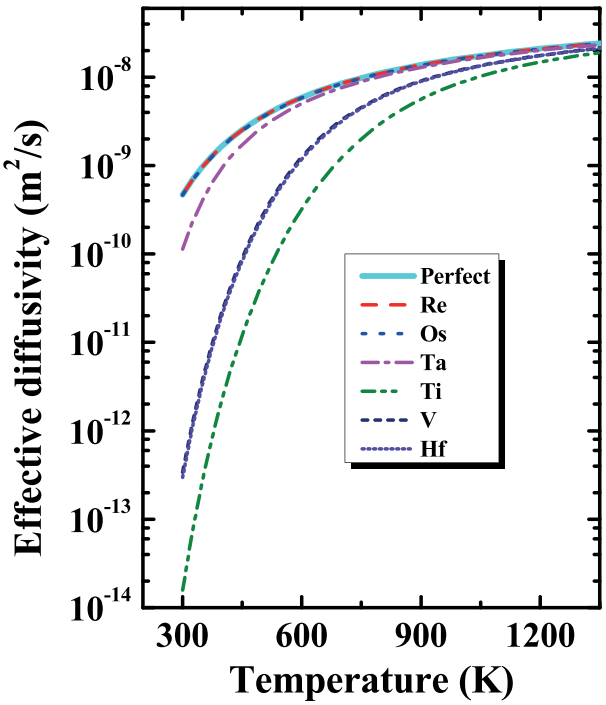

Figure 9. The effective diffusivity of hydrogen in the solid solution of tungsten with a solute concentration 10^{-2}. The diffusivity of hydrogen in perfect tungsten is extracted from [62]. (For an interpretation of the references to colour in this figure legend, the reader is referred to the web version of this article).

atoms has little effect on the hydrogen dissolution in the vacancy. Furthermore, the results on the interaction of the substitutional TM solute atoms with point defects (i.e. the vacancy and self-interstitial) suggests that Re, Os, Ta, Ti, V, and Hf can narrow the gap in the mobility bias between the vacancy and self-interstitial in tungsten, thereby increasing the recombination rate of the vacancy with the self-interstitial. As a result, these solutes should be expected to exert a restraining effect on the growth of the radiation-induced defects and decrease the concentration of defects, particularly the vacancies and vacancy clusters [42]. In this regard, the introduction of these solute atoms should decrease the retention of hydrogen in tungsten. The combination of these findings could provide a good explanation for recent experimental results.

Two typical experimental studies on deuterium retention in tungsten and Re-doped tungsten (W–Re alloy) have been done by Golubeva *et al* and Tyburska-Püschel *et al* [22, 23]. Their results seem to be inconsistent: the former found no difference in deuterium retention in W and W–Re alloys [22]; whereas the later observed a significant reduction of deuterium retention in W–Re alloy relative to pure tungsten [23]. The biggest discrepancy between these two experiments is the difference in the sample pretreatment. Tyburska-Püschel *et al* pre-irradiated their samples with 20 MeV tungsten ions before the deuterium implantation (designated as 'damaged' samples), while Golubeva *et al* did not have a similar treatment (named as 'undamaged' samples). In addition, Golubeva *et al* used a much lower incident deuterium ion flux (5×10^{19} m^{-2} s^{-1}) than Tyburska-Püschel *et al* (10^{22} m^{-2} s^{-1}). The incident deuterium ion energies are both low (200 eV for Golubeva,

76 eV for Tyburska-Püschel). Thus it is reasonable to assume that the material modification of the 'undamaged' samples was minor due to the use of low-energy and low-flux deuterium implantation. Thus, deuterium retention in this case was most probably dominated by trapping on pre-existing defects. As mentioned above, the solute Re has little effect on the hydrogen distribution and diffusivity and cannot act as the hydrogen trapping site. Therefore, the presence of Re in tungsten has little effect on the pre-existing defects concentration of the materials, and then does not influence pronouncedly the deuterium accumulation in the undamaged samples. In the pre-damaged samples, the defects responsible for the trapping of the deuterium are dominated by the high-energy tungsten ion radiation-induced defects, whose concentration would be reduced by the solute Re, as discussed above. Therefore, the deuterium retention is lower in the damaged W–Re alloy than in similarly treated pure tungsten.

A similar explanation can also be applied to the experimental results of deuterium retention in the W-Ta alloy. It has been found that deuterium retention in the W-Ta alloy is significantly higher than in W when the samples are exposed to the deuterium plasma with low energy and low ion flux, while it is lower when the samples are exposed to low energy and high flux deuterium plasma [25–28]. In the case of low ion flux, the deuterium retention is dominated by trapping on pre-existing defects in the material. Since the solute Ta can act as the deuterium trapping site, the introduction of Ta in tungsten would increase the pre-existing defects in materials. Meanwhile, under the condition of high deuterium flux irradiation, the irradiation-induced point defects play a dominate role in deuterium retention, whose concentration could be significantly reduced by the solute Ta.

Based on the influence of these solutes on the radiation-induced defects evolution and their transmutation behaviours, we have suggested that Re might be chosen as a suitable alloying element relative to Ta, Ti and V, and that Ta seems a suitable addition to the W–Re alloy to adjust the concentration of Re and Os [42]. This proposal has also been supported by the interaction between He and these solutes [48, 49]. Here, the influence of these alloying additions on the hydrogen retention also supports this proposal: (i) under normal conditions, Re does not affect the hydrogen distribution and diffusion behaviours in the interstitial site and in the vacancy, while Ta, Ti, and V can trap multiple hydrogen atoms and marginally enhance the ability of the vacancy trapping hydrogen, leading to a significant increase of the hydrogen retention in tungsten; (ii) under irradiation conditions, Re would more effectively promote the recombination of the radiation-induced defects than Ta, V, and Ti. Since the radiation-induced defects are considered as the predominant trapping sites for hydrogen retention, it can be further speculated that Re has a better ability to reduce hydrogen retention in material in a fusion environment. As compared to the Ti and V, Ta has a smaller effect on the increase of hydrogen and helium retention in tungsten and on the acceleration of the radiation-induced defect recombination. The advantage of Ta is that its primary transmutation product is tungsten. The introduction of a certain amount of Ta in the W–Re alloy can serve to adjust the concentration of Re and may suppress the phase precipitation of Re and the irradiation hardening in the W–Re alloy [64].

5. Conclusions

We have performed systematic first-principles calculations to predict the interaction between TM solutes and hydrogen in the interstitial site and the vacancy in tungsten. The main calculated results are as follows.

(i) The interstitial hydrogen site preference of the TIS over the OIS is significantly influenced by the solute atoms. It is enhanced by the substitutional solute with *d* electrons less than tungsten whereas it is weakened by those with *d* electrons more than tungsten. The further electron analysis shows that the charge density perturbation give rise to the site preference changes in the vicinity of the solute atom.

(ii) The solute-H interactions are mostly attractive except for Re; it can be expected that these solute atoms can trap multiple hydrogen atoms to form interstitial hydrogen clusters and impede the hydrogen diffusion. The solute-H interaction is very local, limited within the second nearest neighbour shell, and the presence of a hydrogen atom near the solute atom has a negative effect on the binding of other hydrogen atoms. Both of them would restrict the maximum size of the hydrogen cluster around the solute.

(iii) The solute-H interaction can be well understood in terms of the competition between the elastic and chemical interactions. The elastic interaction is primarily responsible for the solute-H interaction for the TM solutes with small atomic volume and large electronegativity, while the chemical interaction dominates the solute-H interaction for the TM solutes with large atomic volume and small electronegativity.

(iv) The large positive binding energies among the solute, vacancy and hydrogen suggest that they would easily form a defect cluster in tungsten. The results of incremental binding energies show that the solute-H interaction plays a minor role when hydrogen is in the presence of a vacancy, whereas vacancy-H interactions dominate.

Based on our calculations, we estimate the influence of some solute atoms on hydrogen dissolution and diffusion in tungsten. We found that Re and Os exert little effect on the hydrogen distribution and effective diffusivity. Ta, Ti, V, and Hf can trap multiple hydrogen atoms in their neighbouring shells to form many small hydrogen clusters and decrease the hydrogen effective diffusivity, which could, to some extent, prevent the occurrence of large bubbles, but significantly increase the hydrogen retention in tungsten. Together with the influence of these solutes on the radiation-induced defects evolution, these results provide a good explanation for recent experimental results. These results also lend support to our previous proposal that Re might be chosen as a suitable alloying element relative to Ta, Ti and V, and that Ta seems a suitable addition to the W–Re alloy to adjust the concentration of Re and Os.

Acknowledgment

This work was supported by the National Magnetic Confinement Fusion Program (Grant No.: 2015GB112001), the National Natural Science Foundation of China (Nos.: 11505229, 11375231), the Anhui Provincial Natural Science Foundation (No.: 1508085SQE209) and by the Center for Computation Science, Hefei Institutes of Physical Sciences. Q.M. Hu acknowledges the financial support from the MoST of China under grant No. 2014CB644001, from the NSFC under grants Nos. 51171187 and 51271181. The Research Project was part of the CRP carried out under the sponsorship of the IAEA.

References

[1] ITER Physics Basis Editors, ITER Physics Expert Group Chairs, Co-Chairs, ITER Joint Central Team and Physics Integration Unit 1999 *Nucl. Fusion* **39** 2137
[2] Causey R., Wilson K., Venhaus T. and Wampler W.R. 1999 *J. Nucl. Mater.* **266** 467
[3] Skinner C.H. *et al* 2008 *Fusion Sci. Technol.* **54** 891
[4] Roth J. and Schmid K. 2011 *Phys. Scr.* T **145** 014031
[5] Lu G.H., Zhou H.B. and Becquart C.S. 2014 *Nucl. Fusion* **54** 086001
[6] Hu Q.M., Xu D.S., Yang R., Li D. and Wu W.T. 2002 *Phys. Rev.* B **66** 064201
[7] Li Y.J., Kulkova S.E., Hu Q.M., Bazhanov D.I., Xu D.S., Hao Y.L. and Yang R. 2007 *Phys. Rev.* B **76** 064110
[8] Counts W.A., Wolverton C. and Gibala R. 2010 *Acta Mater.* **58** 4730
[9] Counts W., Wolverton C. and Gibala R. 2011 *Acta Mater.* **59** 5812
[10] Nguyen N.B., Lebon A., Vega A. and Mokrani A. 2012 *J. Alloys Compd.* **545** 19
[11] Spiridonova T.I., Tuch E.V., Bakulin A.V. and Kulkova S.E. 2014 *J. Phys.: Conf. Ser.* **552** 012041
[12] Psiachos D., Hammerschmidt T. and Drautz R. 2012 *Comput. Mater. Sci.* **65** 235
[13] Becquart C.S. and Domain C. 2012 *Curr. Opin Solid State Mater. Sci.* **16** 115
[14] Jin S., Liu Y.L., Zhou H.B., Zhang Y. and Lu G.H. 2011 *J. Nucl. Mater.* **415** S709
[15] Kato D., Iwakiri H., Morishita K. and Muroga T. 2011 *Plasma Fus. Res.* **6** 2405062
[16] Ou X.D., Shi L.Q., Sato K., Xu Q. and Wang Y.X. 2012 *Nucl. Fusion* **52** 123003
[17] Liu N., Huang J., Sato K., Xu Q., Shi L.Q. and Wang Y.X. 2014 *Nucl. Fusion* **54** 033013
[18] Kong X.S., You Y.W., Fang Q.F., Liu C.S., Chen J.L., Luo G.N., Pan B.C. and Wang Z. 2013 *J. Nucl. Mater.* **433** 357
[19] Wang S., Kong X.S., Wu X.B., Fang Q.F., Chen J.L., Luo G.N. and Liu C.S. 2015 *J. Nucl. Mater.* **459** 143
[20] Heinola K., Ahlgren T., Nordlund K. and Keinonen J. 2010 *Phys. Rev.* B **82** 094102
[21] Gilbert M.R. and Sublet J.C. 2011 *Nucl. Fusion* **51** 043005
[22] Golubeva A.V., Mayer M., Roth J., Kurnaev V.A. and Ogorodnikova O.V. 2007 *J. Nucl. Mater.* **363–5** 893
[23] Tyburska-Püschel B. and Alimov V.K. 2013 *Nucl. Fusion* **53** 123021
[24] Alimov V.K., Hatano Y., Sugiyama K., Balden M., Oyaidzu M., Akamaru S., Tada K., Kurishita H., Hayashi T. and Matsuyama M. 2014 *J. Nucl. Mater.* **454** 136
[25] Schmid K., Rieger V. and Manhard A. 2012 *J. Nucl. Mater.* **426** 247
[26] Zayachuk Y., 't Hoen M.H.J., van Emmichoven P.A.Z., Uytdenhouwen I. and Van Oost G. 2012 *Nucl. Fusion* **52** 103021
[27] Zayachuk Y., 't Hoen M.H.J., van Emmichoven P.A.Z., Terentyev D., Uytdenhouwen I. and Van Oost G. 2013 *Nucl. Fusion* **53** 013013
[28] Zayachuk Y., Manhard A., 't Hoen M.H.J., Jacob W., van Emmichoven P.A.Z. and Van Oost G. 2014 *Nucl. Fusion* **54** 123013
[29] Myers S.M. *et al* 1992 *Rev. Mod. Phys.* **64** 559
[30] Matsumoto T. 1977 *J. Phys. Soc. Japan* **42** 1583
[31] Westlake D.G. and Miller J.F. 1979 *J. Less-Common Met.* **65** 139
[32] Miller J.F. and Westlake D.G. 1980 *Trans. Japan. Inst. Met.* **21** 153
[33] Lauf R.J. and Altstetter C.J. 1979 *Acta Metall.* **27** 1157
[34] Liu P., Xing W., Cheng X., Li D., Li Y. and Chen X.Q. 2014 *Phys. Rev.* B **90** 024103
[35] Rieth M. *et al* 2013 *J. Nucl. Mater.* **432** 482
[36] Wurster S. *et al* 2013 *J. Nucl. Mater.* **442** S181
[37] Fukuzumi S., Yoshiie T., Satoh Y., Xu Q., Mori H. and Kawai M. 2005 *J. Nucl. Mater.* **343** 308
[38] Kresse G. and Hafner J. 1993 *Phys. Rev.* B **47** 558–61
[39] Kresse G. and Furthmuller J. 1996 *Phys. Rev.* B **54** 11169–86
[40] Blöchl P.E. 1994 *Phys. Rev.* B **50** 17953
[41] Perdew J.P. *et al* 1992 *Phys. Rev.* B **46** 6671
[42] Kong X.S., Wu X.B., You Y.W., Liu C.S., Fang Q.F., Chen J.L., Luo G.N. and Wang Z. 2014 *Acta Mater.* **66** 172
[43] Liu Y.L., Zhang Y., Zhou H.B., Lu G.H., Liu F. and Luo G.N. 2009 *Phys. Rev.* B **79** 172103
[44] Heinola K. and Ahlgren T. 2010 *J. Appl. Phys.* **107** 113531
[45] Ohsawa K., Goto J., Yamakami M., Yamaguchi M. and Yagi M. 2010 *Phys. Rev.* B **82** 184117
[46] Jiang B., Wang F.R. and Geng W.T. 2010 *Phys. Rev.* B **81** 134112
[47] Nguyen-Manh D. 2009 *Adv. Mater. Res.* **59** 253
[48] Wu X.B., Kong X.S., You Y.W., Liu C.S., Fang Q.F., Chen J.L., Luo G.N. and Wang Z. 2014 *J. Nucl. Mater.* **455** 151
[49] Wu X.B., Kong X.S., You Y.W., Liu C.S., Fang Q.F., Chen J.L., Luo G.N. and Wang Z.G. 2013 *Nucl. Fusion* **53** 073049
[50] Henriksson K.O.E. *et al* 2005 *Appl. Phys. Lett.* **87** 163113
[51] Becquart C.S. and Domain C. 2009 *J. Nucl. Mater.* **386–8** 109
[52] Liu Y.L., Zhang Y., Luo G.N. and Lu G.H. 2009 *J. Nucl. Mater.* **390–1** 1032
[53] Haasz A.A., Poon M. and Davis J.W. 1999 *J. Nucl. Mater.* **266–9** 520
[54] Wang W., Roth J., Lindig S. and Wu C.H. 2001 *J. Nucl. Mater.* **299** 124
[55] Gschneidner K.A. 1964 *Solid State Phys.* **16** 275
[56] Olsson P., Klaver T.P.C. and Domain C. 2010 *Phys. Rev.* B **81** 054102
[57] Henkelman G., Arnaldsson A. and Jnsson H. 2006 *Comput. Mater. Sci.* **36** 354
[58] Sanville E., Kenny S.D., Smith R. and Henkelman G. 2007 *J. Comput. Chem.* **28** 899
[59] Gumbsch P. 2003 *J. Nucl. Mater.* **323** 304
[60] Hirai T., Pintsuk G., Linke J. and Batilliot M. 2009 *J. Nucl. Mater.* **390–1** 751
[61] Simonovic D., Ande C.K., Duff A.I., Syahputra F. and Sluiter M.H.F. 2010 *Phys. Rev.* B **81** 054116
[62] Kong X.S., Wang S., Wu X.B., You Y.W., Liu C.S., Fang Q.F., Chen J.L. and Luo G.N. 2015 *Acta Mater.* **84** 426
[63] Oriani R.A. 1970 *Acta Metall.* **18** 147
[64] Xu A., Beck C., Armstrong D.E.J., Rajan K., Smith G.D.W., Bagota P.A.J. and Roberts S.G. 2015 *Acta Mater.* **87** 121